Tuning Two Interfaces with Fluoroethylene Carbonate Electrolytes for High-Performance Li/LCO Batteries

Jinhong Lee,[†] Yun-Jung Kim,[†] Hyun Soo Jin,[†] Hyungjun Noh,[†] Hobeom Kwack,[†] Hyunwon Chu,[†] Fangmin Ye,[†,‡] Hongkyung Lee,[§] and Hee-Tak Kim*,[†,‡]

[†]Department of Chemical and Biomolecular Engineering, Korea Advanced Institute of Science and Technology, 291 Daehak-ro, Yuseong-gu, Daejeon 34141, Republic of Korea

[‡]Advanced Battery Center, KAIST Institute for the NanoCentury, Korea Advanced Institute of Science and Technology, 335 Gwahangno, Yuseong-gu, Daejeon 34141, Republic of Korea

[§]Energy and Environment Directorate, Pacific Northwest National Laboratory, 902 Battelle Boulevard, Richland, Washington 99352, United States

S *Supporting Information*
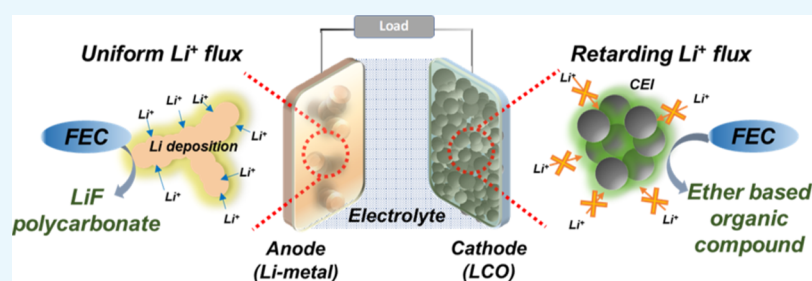
ABSTRACT: Various electrolytes have been reported to enhance the reversibility of Li-metal electrodes. However, for these electrolytes, concurrent and balanced control of Li-metal and positive electrode interfaces is a critical step toward fabrication of high-performance Li-metal batteries. Here, we report the tuning of Li-metal and lithium cobalt oxide (LCO) interfaces with fluoroethylene carbonate (FEC)-containing electrolytes to achieve high cycling stability of Li/LCO batteries. Reversibility of the Li-metal electrode is considerably enhanced for electrolytes with high FEC contents, confirming the positive effect of FEC on the stabilization of the Li-metal electrode. However, for FEC contents of 50 wt % and above, the discharge capacity is significantly reduced because of the formation of a passivation layer on the LCO cathodes. Using balanced tuning of the two interfaces, stable cycling over 350 cycles at 1.5 mA cm^{-2} is achieved for a Li/LCO cell with the 1 M LiPF$_6$ FEC/DEC = 30/70 electrolyte. The enhanced reversibility of the Li-metal electrode is associated with the formation of LiF and polycarbonate in the FEC-derived solid electrolyte interface (SEI) layer. In addition, electrolytes with high FEC contents lead to lateral Li deposition on the sides of Li deposits and larger dimensions of rodlike Li deposits, suggesting the elastic and ion-conductive nature of the FEC-derived SEI layer.

INTRODUCTION

Rechargeable lithium-metal batteries have received great attention because of their great potential to achieve high energy density based on the low redox potential (−3.04 V vs standard hydrogen electrode) and high theoretical capacity (3860 mA h g^{-1}) of the Li metal.[1−4] Coupled with a high capacity cathode such as a sulfur and oxygen cathode, a Li-metal anode can provide a specific energy density higher than those possible with lithium-ion batteries.[5−8] However, the practical use of the Li metal for rechargeable batteries has not yet been fully realized because of the deep-rooted problems of chronic Li dendrite growth and poor Li-metal Coulombic efficiency (CE).[9,10] The irreversible reaction between the lithium metal and organic electrolyte can be mitigated by forming a stable interface layer; with exposure of a lithium-metal anode to an organic electrolyte, the decomposition of the electrolyte results in the formation of a passivation layer

called a solid electrolyte interface (SEI), ideally preventing further reaction between the organic electrolyte and lithium-metal anode.[1,11] However, the original SEI layers are broken during the severe lithium striping/plating process, and new SEI layers are formed on the fresh lithium surface with continuous consumption of the electrolyte and Li metal. As the result of the repetition of these processes, the uneven SEI layers are piled up to form a thick layer on the surface of the Li-metal anode, called a porous layer, which creates a large resistance and eventually leads to cell failure.[12−15] In the case of a silicon and graphite anode, this uneven and resistive SEI layer formation has been a critical issue for cycling stability.[16−18] To prevent the electrolyte decomposition and Li dendrite

Scheme 1. FEC-Based Electrolyte Decomposition Process on Anode and Cathode Surfaces
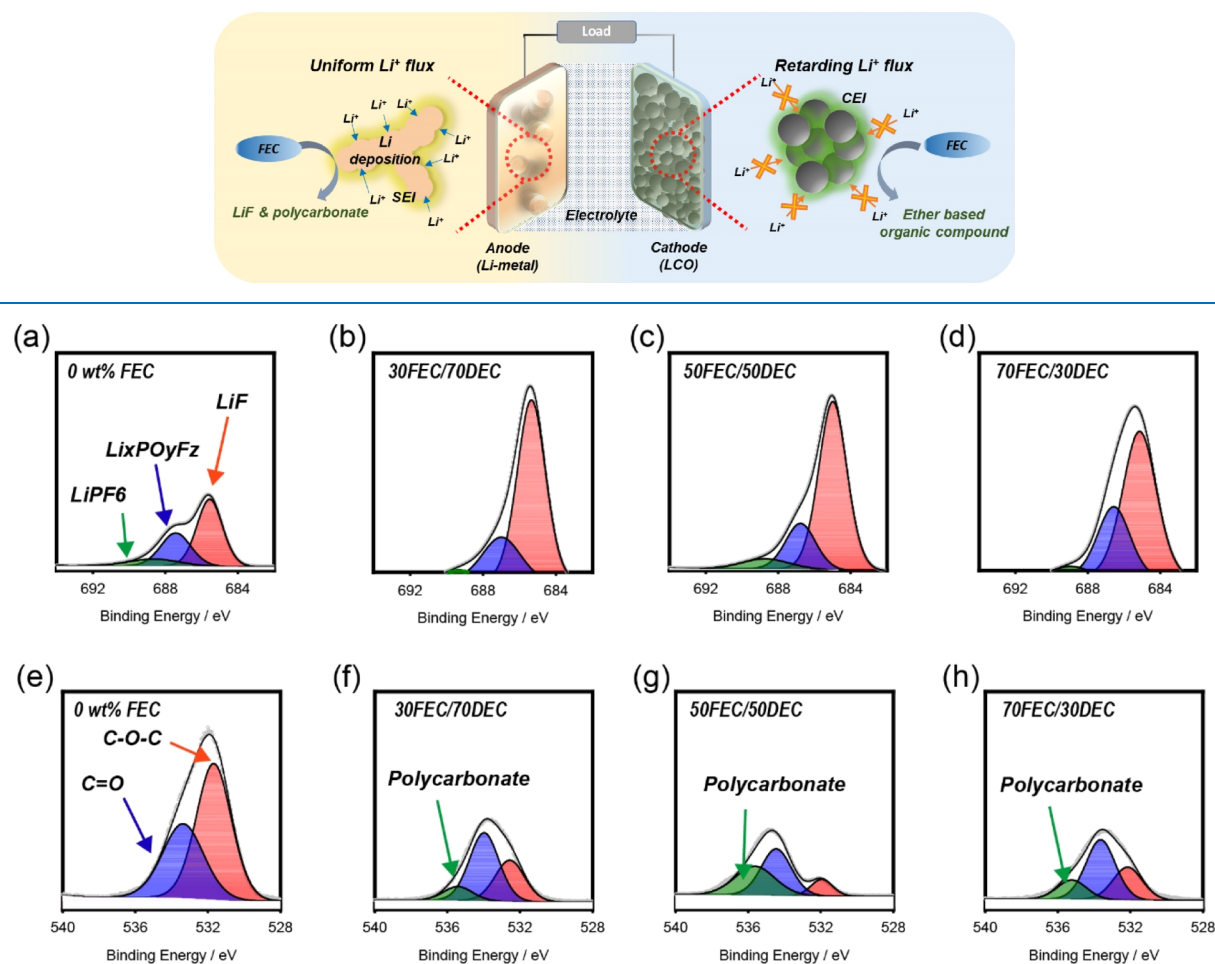

Figure 1. (a−d) F 1s XPS analysis and (e−h) O 1s XPS spectra of the Li-metal electrode surfaces after 10 cycles for Li/Li symmetric cells with control, 30FEC/70DEC, 50FEC/50DEC, and 70FEC/30DEC electrolytes.

formation, coating of a polymer composite protective layer[19,20] or silicon nanoparticles[21] on the Li-metal anode has been suggested. These approaches exploit the high shear modulus of ceramic particles to mechanically suppress the growth of the Li dendrite.[22,23] However, because of the existence of soft Li-ion conducting phases or defects and consequent penetration of the Li dendrite through them, the artificial protective layers do not perfectly prevent Li dendrite growth. The other strategy is to form a stable SEI layer using an electrolyte additive such as fluoroethylene carbonate (FEC),[24] vinylidene carbonate,[25] LiNO$_3$[26] and polysulfides.[27] These additives preferentially decompose on the Li-metal surface, forming a robust SEI layer. The unique benefit of the additive approach is that the defect in the SEI layer can be healed by the remaining additives in the electrolytes until additives are totally consumed. Among these additives, FEC is most widely known as particularly effective at stabilizing lithium-metal anodes, as well as silicon or graphite anodes; its ability to do this is attributed to the formation of an SEI layer having Li-ion-conducting LiF and elastic polycarbonate; LiF has an ionic conductivity of 10^{-7} to 10^{-13} S cm^{-1},[28] and the polycarbonate imparts a flexibility to the SEI layer, that is required to accommodate the significant volume change of the lithium-metal and silicon anode.[29] However, for Li metal and silicon anodes, the FEC additive approach does not achieve long cycling stability due to the early consumption

of FEC.[30] Considering this limitation, the Zhang group proposed an electrolyte comprising FEC solvent and LiNO$_3$, which participate in Li solvation sheath for making a stable SEI layer.[31] In addition, Aurbach's group used FEC as a main solvent and demonstrated an extended cycling stability for silicon anodes with the FEC/DMC electrolyte.[32] Very recently, they reported that the FEC/DMC-based electrolyte system is also effective for lithium-metal batteries;[33] an Li/Li symmetric cell with the FEC-based electrolyte was cycled at 2 mA cm^{-2} for more than 1100 cycles. Moreover, the FEC-based electrolyte was used for practical loading of the NCM cathode about 3.3 mA h cm^{-2}.[34] However, they did not clarify in detail the negative effects of the FEC solvent for use in the cathode-electrode interface.

In this work, we report the tuning of the Li metal and lithium cobalt oxide (LCO) interface with FEC-containing electrolytes to achieve a Li/LCO battery with excellent cycling stability. Ionic conductivity measurement and cycling tests for Li/Cu and Li/LCO cells were conducted with the FEC-containing electrolytes to verify the positive effect of FEC on Li-metal stabilization. We also assessed the compatibility with the LCO cathode of the FEC-containing electrolytes. To deepen the understanding of the SEI layer derived from FEC-based electrolytes and the resulting Li deposit morphology, X-ray photoelectron spectroscopy (XPS), impedance, and
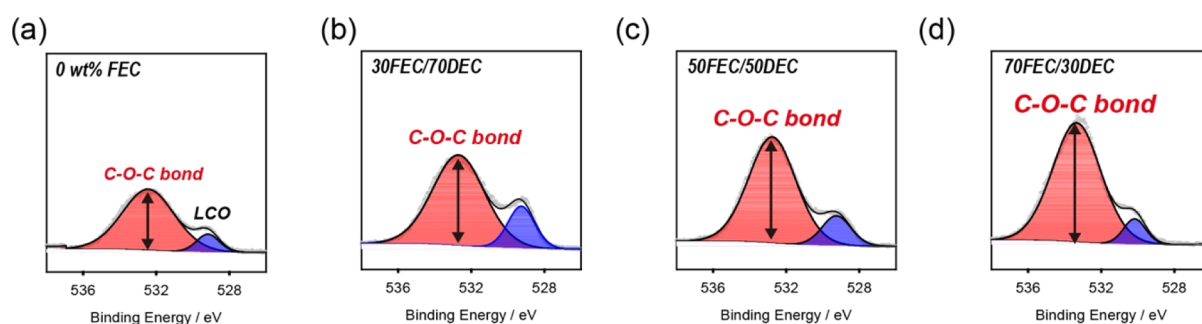
Figure 2. O 1s XPS analysis of the LCO cathode electrode surfaces after 10 cycles for the Li/LCO half cells with (a) 0 wt % FEC, (b) 30FEC/70DEC, (c) 50FEC/50DEC, and (d) 70FEC/30DEC electrolyte.

scanning electron microscopy (SEM) analyses were carried out. This contribution will emphasize the importance of the control of both LCO and Li interfaces to achieve high-performance lithium-metal batteries with an FEC-based electrolyte, and of the formation of an ion-conductive and elastic SEI layer with FEC-based electrolytes to enhance the reversibility of the Li-metal electrode.

■ RESULTS AND DISCUSSION

Scheme 1 depicts the FEC decomposition process on Li-metal anode and LCO cathode surfaces. On the anode side, because of the highly reactive Li-metal, the FEC-contained electrolyte is decomposed to form an SEI. The SEI from FEC is mainly composed of LiF and polycarbonate; LiF is well known to induce uniform Li-ion flux on the surface and the polycarbonate to impart flexibility to the SEI.[2] The uniform Li^+ flux through the LiF-containing SEI layer can suppress the growth of Li dendrites because the lithium dendrite growth is accelerated because of locally concentrated Li^+ flux. In addition, by mechanically suppressing the dendrite growth in the opposite direction, the polycarbonate component enables the SEI layer to accommodate severe volume change of the Li-metal. Therefore, decomposed FEC compounds such as LiF and polycarbonate simultaneously prohibit dendrite growth by forming a stable SEI on the Li metal. However, the FEC can be decomposed on a cathode on which a resistive cathode electrolyte interface (CEI) such as an ether-based organic compound is created. This CEI retards lithium-ion conduction to the cathode-active material. Therefore, tuning the two interfaces of the anode and the cathode, by adjusting the amount of the FEC solvent, is important for advanced Li-metal batteries. The increasing amount of FEC in the electrolyte is good for the anode electrode, producing a stable SEI on the Li metal. However, a large amount of FEC in the electrolyte accelerates the decomposition of FEC on the cathode and produces resistive ether-based organic compounds. Therefore, for the design of FEC-based electrolytes, FEC/diethylene carbonate (DEC) ratios were varied at 30/70, 50/50, and 70/30 in the volume ratio, with 1 M $LiPF_6$ salt; these mixtures are denoted 30FEC/70DEC, 50FEC/50DEC, and 70FEC/30DEC, respectively; 1 M $LiPF_6$ EC/DEC (50/50) electrolyte was used as a control sample (0 wt %FEC).

As the FEC decomposed on the Li-metal by reduction reaction, the FEC content effect was also observed, which could be related with the chemical component change of the SEI layer of the Li-metal electrode. A series of XPS analyses was conducted to characterize the SEI layer formed with these electrolytes. After 10 iterations of galvanostatic cycling at 1 mA

cm^{-2}, the XPS spectra of the washed Li-metal surfaces were taken. As shown in Figure 1a−d, the F 1s spectra for the control electrolyte and three FEC-based electrolytes (30FEC/70DEC, 50FEC/50DEC, and 70FEC/30DEC) showed three main peaks at 685.0, 687.0, and 689.5, which correspond to LiF, $Li_xPO_yF_z$, and $LiPF_6$, respectively. The LiF and $Li_xPO_yF_z$ peaks may come from the decomposition of the $LiPF_6$ lithium salt, and the $LiPF_6$ peak from the residual $LiPF_6$ salt.

Compared with the control, the FEC/DEC electrolytes exhibited stronger LiF peaks; the peak intensity ratios of the peak height of the $Li_xPO_yF_z$ and LiF peaks were considerably lower for the FEC/DEC electrolytes than for the control. Because $Li_xPO_yF_z$ originates from the decomposition of $LiPF_6$, and LiF from both $LiPF_6$ and FEC, the lower peak intensity ratios indicate that FEC strongly contributes to the formation of the SEI layer for the FEC/DEC electrolytes. Therefore, the fluorine atomic percentage of the FEC/DEC electrolyte was higher than that of the control electrolyte in Figure S1. According to previous works on FEC-derived SEI layers, FEC is decomposed into LiF and vinyl carbonate (VC), and the VC is polymerized to form polycarbonate on lithium metal, graphite, and silicon anode material.[35] Therefore, the relatively high intensity of the LiF peak for the FEC/DEC electrolytes can be understood. Figure 1e−h shows the O 1s XPS spectra of the lithium-metal surfaces after 10 cycles. For the control electrolyte, two major peaks at 531.5 and 533.5 eV were observed, which correspond to carbonyl oxygen and ether oxygen groups of $LiOCO_2R$, respectively. The higher intensities of the $LiOCO_2R$ peak for the control electrolyte indicate that the decomposition of EC- and DEC-free solvents was more severe than the case for the FEC/DEC electrolytes. On the other hand, the O 1s XPS spectra for the FEC/DEC electrolytes showed a new peak at 535.5 eV, which corresponds to the −COO− group from polycarbonate, together with the other two peaks. The peak from polycarbonate again supports the contribution of FEC on the SEI layer formation.

To investigate the FEC effect on the cathode, chemical analysis of the cathode is necessary. The oxidation potential of FEC has been reported by density functional theory calculation to be 7.24 V, which is higher than that of EC (6.95 V). However, in a real cell system, the oxidation of EC and FEC can be expected at a lower potential because of nucleophilic attacks of the cathode surface oxygen atoms.[36] Generally, the anion salt in the electrolyte coordinates more with the free solvent, which has a higher dielectric constant. Therefore, the $PF6^-$ anion salt easily coordinates with the FEC electrolyte and then provides the negative charge to the coordinated solvent, which reaches the cathode electrode more easily than does the other solvent, resulting in the preferential reaction of

FEC during the charging process.[37] Therefore, a much greater amount of the FEC solvent can be decomposed on the cathode side than when using the EC and DEC solvents.

To understand the side reaction between the FEC-based electrolyte and the LCO cathode, we used XPS to analyze the LCO cathode after 10 cycles. As shown in Figure 2a–d, the O 1s spectra of the LCO cathodes reveal two major peaks centered at 529 and 533 eV that correspond to the oxygen in the metal oxide (LCO) and to the ether group (C−O−C), respectively. Unlike the control sample shown in Figure 2a, the intensities of the ether group (C−O−C) signal for the FEC-containing electrolyte were strong, as observed in the O 1s XPS analysis. From the result showing that the intensity of ether compounds such as poly(ethylene oxide) organic compounds increases with increasing the FEC content, we can conclude that FEC has a great influence on the formation of the resistive CEI on the cathode surface. Therefore, the decomposition of FEC on the cathode can be attributed to the Li/LCO cell performance, such as the degree of discharge capacity and the capacity retention. In addition, the F 1s and C 1s spectra of LCO are shown in Figure S2, respectively. From the F 1s spectra, the peaks from LiF (685 eV) and from $Li_xPO_yF_z$ (687 eV) were identified. The stronger LiF and $Li_xPO_yF_z$ peaks observed for the FEC/DEC electrolytes are attributed to the formation of the CEI layer from the FEC solvent. In C 1s spectra, the peak from the ether bond (287 eV) was gradually increased with the FEC content, supporting the formation of the ether-based CEI layer. For further analysis of the electrolyte decomposition at the cathode, Fourier transform infrared (FT-IR) analysis is conducted (Figure S3). As shown in the FT-IR graph, there is one strong characteristic bond at the position of 1143 cm^{-1} for the C−O−C stretching vibration of ether bonding, which commonly lies in the range of 1250−1000 cm^{-1}.[38] The peak of the C−O bond from the ether compound chemicals increased gradually with increasing the FEC content. This observation of the greater amount of the ether compound in the high FEC electrolyte coincides with the XPS results.

Achieving a high ionic conductivity is an important electrolyte design issue; high degree of salt dissociation and high Li-ion mobility are the two requirements for high ionic conductivity.[39] By considering the balance between salt dissociation and Li-ion mobility, a mixture of ethylene carbonate (EC) having a high dielectric constant of 89.0 and a linear carbonate having low viscosity is conventionally used for Li-ion batteries. For this reason, we selected DEC, having a viscosity of 0.75 cps, as a low viscosity co-solvent for the FEC-based electrolyte; we used 1 M $LiPF_6$ EC/DEC (5/5) electrolyte as a control sample (50EC/50DEC). In the design of FEC-based electrolytes, FEC imparts a high dissociation of Li salt, as EC does. The FEC/DEC ratios were varied among 30/70, 50/50, and 70/30 in volume; these samples are denoted as 30FEC/70DEC, 50FEC/50DEC, and 70FEC/30DEC, respectively. In addition, EC/DEC electrolytes with FEC additives were also prepared; FEC was added to the control electrolyte at 2 and 10 wt %.

Ionic conductivities of these electrolytes were measured from the impedances of the corresponding symmetric cells. As shown in the Nyquist plots of the impedances (Figure S4a), the FEC-containing electrolytes showed much smaller Ohmic resistances compared with the control EC/DEC electrolyte and the electrolytes with variation of the FEC content. From the Ohmic resistances and the thickness of the porous

separator, the ionic conductivities of the electrolyte-filled separator were determined and are compared in Figure S4b. The control electrolyte has an ionic conductivity of 1.5×10^{-3} S cm^{-1}, which is approximately two times lower than those for the 2 and 10 wt % FEC-containing 50EC/50DEC electrolytes. Because the dielectric constant of FEC (110) is higher than that of EC, the FEC-containing electrolytes have stronger Li-ion solvation power than does the control, which explains the higher ion conductivities. The FEC/DEC electrolytes also showed higher ionic conductivities: 4.79, 4.37, and 3.78×10^{-3} S cm^{-1} for 30FEC/70DEC, 50FEC/50DEC, and 70FEC/30DEC, respectively. The ion conductivity decreased with increasing the FEC content for the FEC/DEC electrolytes and FEC additive-containing EC/DEC electrolytes; this is attributed to the increased electrolyte viscosity with increasing the FEC content. Therefore, the use of FEC as an additive or co-solvent is highly beneficial in attaining high ionic conductivity, and the 30FEC/70DEC electrolyte has the highest ionic conductivity among all samples. Furthermore, for investigating the wettability of the electrolytes with the separator, we measured the contact angle of the liquid electrolyte on the polypropylene (PP) separator by optical microscopy (Figure S5). A lower contact angle means a poorer wettability with the separator. The control, 30FEC/70DEC, 50FEC/50DEC, 70FEC/30DEC, and 90FEC/10DEC electrolyte showed a contact angle of 155°, 154°, 152°, 150°, and 138°, respectively. For the FEC content of 70% and below, the contact angles are nearly invariant, indicating similar wettability. On the other hand, the relatively low contact angle for the 90FEC/10DEC electrolyte suggests poorer wettability. Therefore, the FEC-containing electrolytes do not practically suffer from the electrolyte wetting problem at the FEC content of 70% or below.

To examine the reversibility of the lithium stripping/plating process for the electrolytes, galvanostatic cycling experiments were conducted with the corresponding Li−Cu half-cells. Li-metal plating on the Cu electrode was conducted at 1 mA cm^{-2} for 1 h and Li stripping from the Li deposit was carried out at the same current density. According to the voltage profiles during the plating/stripping (Figure 3a), the FEC-containing electrolytes exhibited larger stripping capacity than the control electrolyte, indicating an improved reversibility. The CE at the first cycle was 87.6, 95.4, 91.3, 93.8, 93.8, 96.1, and 96.0% for the control (0 wt % FEC), 2 wt % FEC, 10 wt % FEC, 30FEC/70DEC, 50FEC/50DEC, and 70FEC/30DEC, respectively.
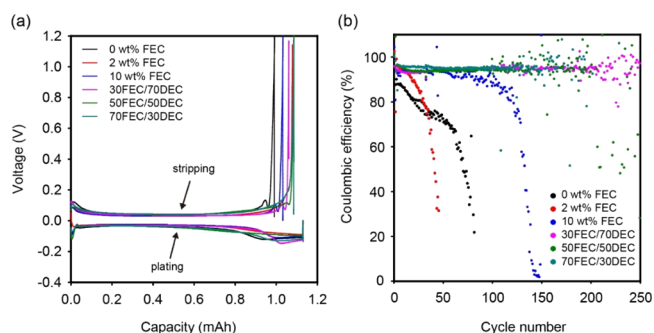
Figure 3. (a) Voltage profiles at the first galvanostatic charge and discharge cycle of the Li/Cu cells with 0 wt % FEC (control), 2 wt % FEC, 10 wt % FEC, 30FEC/70DEC, 50FEC/50DEC, and 70FEC/30DEC electrolytes. (b) CEs of the Li/Cu cells as a function of the cycle number measured at 1 mA cm^{-2} and 1 mA h cm^{-2}.
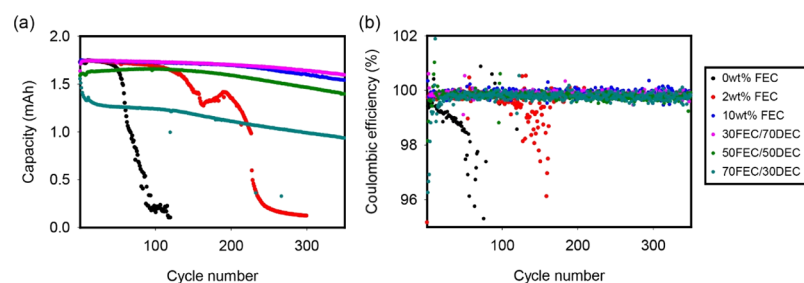
Figure 4. Galvanostatic cycling of Li/LCO and cells with different electrolytes. Plot of (a) discharge capacities and (b) CEs of the Li/LCO cells cycled at 1.0 C rate as a function of the cycle number.

These results clearly indicate that the FEC-containing electrolytes have better reversibility for Li plating/stripping on Cu than does the control electrolyte.

The long-term cycling stability of the Li plating/stripping process was assessed for the electrolytes; the CEs were measured during an extended cycle number, as shown in Figure 3b. The CE of the control electrolyte dramatically decreased after 10 cycles, which means that the control electrolyte is highly unstable with the Li-metal electrode. The addition of FEC additive at 2 and 10 wt % to the control electrolyte resulted in 2 and 3 times improvement of the cycling stability, respectively. For the FEC/DEC electrolytes, the cycling stabilities considerably improved compared with that of the control electrolyte and were even better than those of the FEC additive-containing electrolytes. Among those three FEC/DEC electrolytes, the 30FEC/70DEC electrolyte showed better cycling stability than did the 50FEC/50DEC and 70FEC/30DEC electrolytes; CE for the 30FEC/70DEC electrolyte was maintained at a 95.5% value even after 200 cycles. The averaged CEs for the initial 60 cycles are compared in Table S1 for the FEC/DEC electrolytes. The CEs were considerably higher for the electrolytes with high a FEC content (EC/DEC + 10 wt % FEC and FEC/DEC electrolytes) than for the control or the control with 2 wt % FEC electrolyte. This suggests that a stable SEI can be made when the FEC content exceeds a certain value. We believe that the best cycling stability, observed for the 30FEC/70DEC electrolyte, is attributed to the highest ionic conductivity and the high stability of the corresponding SEI layer. When the ionic conductivity is low, Li$^+$ flux is concentrated at defects or specific sites with lower surface resistance, resulting in uneven Li deposition/plating and consequently low cycling stability.[40]

To demonstrate the applicability of the FEC-containing electrolytes for lithium-metal batteries, we employed Li metal/LCO cells. Figure 4a compares the discharge capacities of Li/LCO cells with the control and FEC-containing electrolytes. The Li/LCO cell with the control electrolyte showed poor capacity retention; the discharge capacity dramatically decreased after the 60th cycle at 1.5 mA cm^{-2} current density (1 C). As shown in Figure 4b, the CE of the LCO cell with the control electrolyte decreased after the 60th cycle; this result strongly correlates with the discharge capacity results. The 2 wt % FEC-containing EC/DEC electrolyte exhibited an improved capacity retention and higher CE (>99%) retention up to the 100th cycle compared with the control cell (Figure 4a,b); however, the cell eventually showed significant capacity, and CE fades after the 150th cycle. Comparison of the 2 and 10 wt % FEC-containing electrolytes shows that the capacity retention and reversibility were highly enhanced with the increase of the FEC content from 2 to 10 wt %. Even at the

350th cycle, the 10 wt % FEC-containing electrolyte maintained 89.3% of its initial capacity with a CE of 98%, which suggests the formation of a highly stable SEI layer. For the FEC/DEC electrolytes, the discharge capacity strongly depended on the FEC content; with increasing the FEC content, the initial discharge capacity decreased. Interesting to us was that the 30FEC/70DEC electrolyte delivered a high initial discharge capacity, comparable to that of the control, and an excellent capacity retention of 97.5% at the 350th cycle, with a CE of 99.8%. At an FEC content of 50% and above, the CEs in early cycling were quite unstable, indicating the occurrence of a side reaction. Although the electrolytes showed high cycling stability of the Li-metal electrode, side reaction of FEC at the LCO cathode may cause the lower initial discharge capacities.[41] To verify the FEC decomposition and consequent LCO passivation for the electrolytes with high FEC contents, we also conducted a three-electrode impedance analysis for the Li/LCO cells with the control and 70FEC/30DEC electrolytes. As shown in Figure S6a, the cathode impedances for the control and 70FEC/30DEC electrolytes in the fully charged state after the first cycle exhibited two semicircles; the high frequency (500 Hz) and low frequency (5 Hz) semicircles are associated with Li$^+$ ion migration through a CEI film and with the charge-transfer process, respectively. The diameters of the high frequency and low frequency semicircles correspond to SEI film resistance and charge-transfer resistance, respectively.[42] The comparison of the control and 70FEC/30DEC electrolytes clearly shows that the SEI film resistance of 70FEC/30DEC is much larger than that of the control, supporting the formation of a more resistive SEI layer for 70FEC/30DEC. The XPS and impedance results collectively suggest that the small discharge capacity of the 70FEC/30DEC electrolyte originate from the SEI formation at the cathode. As shown in Figure S6b, the impedances after the 1st and 30th cycles were nearly identical, which informs that the CEI layer is stably preserved during the cycling after being formed at the first cycle. Although the discharge capacities of the 50FEC/50DEC and 70FEC/DEC electrolytes were smaller because of the CEI formation, their cycling stabilities were quite high, as shown in Figure 4a, because of their Li-metal electrode stabilization. As a result of the balanced SEI control for the Li metal and LCO electrodes, the LCO cell with the 30FEC/70DEC electrolyte showed high initial capacity and the highest capacity retention.

For a deeper understanding of the excellent capacity retention of the 30FEC/70DEC electrolyte, we investigated the evolution of the Li-metal electrode impedance with cycling for Li/LCO cells with control and 30FEC/70DEC electrolytes. A Li-metal reference electrode was inserted into the cell for the analysis. As shown in Figure 5a, the Li-metal electrode
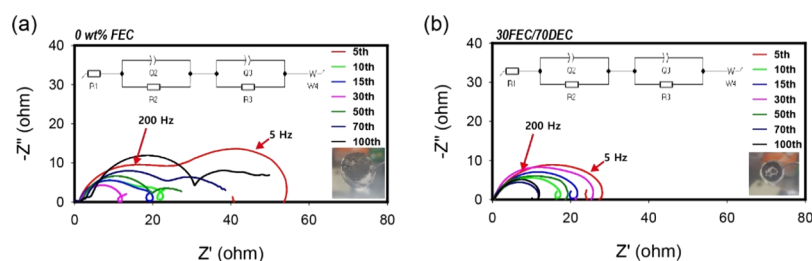
Figure 5. Nyquist plots of the impedances of the Li-metal electrodes in three-electrode configuration measured at various cycles for (a) control electrolyte and (b) 30FEC/70DEC electrolyte. (Inset: Photo images of a lithium-metal anode after 100 cycles).
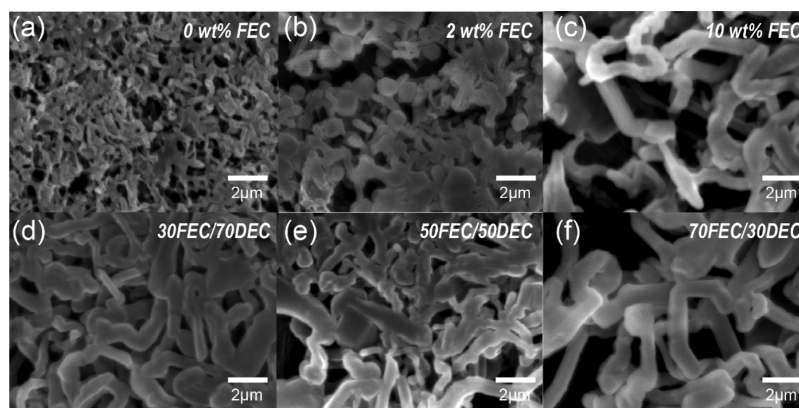
Figure 6. SEM image of the lithium-metal electrode surface after 10 cycles for Li/Li symmetric cells with (a) 0 wt % FEC, (b) 2 wt % FEC, (c) 10 wt % FEC, (d) 30FEC/70DEC, (e) 50FEC/50DEC, and (f) 70FEC/30DEC electrolytes.

impedances for the control electrolyte are featured by two partially overlapped semicircles. According to previous publications, the high-frequency semicircle (200 Hz) is assigned to Li-ion conduction through the SEI layer and the low frequency semicircle (3 Hz) is assigned to charge-transfer process.[43] A circuit model used for the assignment is given in the figures for a better understanding. The size of the semicircles decreased considerably with the cycle in early cycling because inhomogeneous Li deposition/dissolution accompanies an expansion of the Li-metal electrode surface. However, after the 30th cycle, the interfacial and charge-transfer impedances dramatically increased, which indicates the filing up of the resistive porous layers on the lithium-metal surfaces. The inset photo of the lithium-metal surface after 100 cycles clearly shows the porous layer. On the other hand, as shown in Figure 5b, the lithium-metal electrode impedances for the 30FEC/70DEC electrolyte system were quite different from those for the control. The two semicircles were highly overlapped, and the overall magnitudes of the merged semicircles were considerably smaller than those for the control. More importantly, the impedances were stably maintained with the cycle. These results suggest that the SEI layer of the Li-metal electrode derived from FEC is quite stable even for the Li/LCO cell. As shown in the inset, the porous layer formed on the lithium-metal surface after 100 cycles was thinner than that for the control.

For the control and FEC-containing electrolytes, the positive effect of FEC on the stabilization of the Li-metal electrode motivated us to investigate the morphology of the Li-metal electrode after cycling. Although the relationship between the SEI layer and the resulting Li morphology has not been made clear yet, we expect that the Li-ion conductivity and the mechanical property of the SEI layer are critical in the evolution of the Li-metal morphology during repeated cycling. A highly ion-conductive and elastic SEI layer would permit Li deposition under the SEI layer and could withstand the resulting volume expansion to some extent, resulting in thicker and larger Li deposits. After 10 cycles at 1 mA cm^{-2} and 1 mA h cm^{-2}, the Li/Li symmetric cells were disassembled and the surface of the cycled Li-metal electrodes were observed using SEM. As shown in Figure 6a, for the control electrolyte, submicron-sized mossy and needle-like Li dendrites were observed. According to the Li morphology, it appears that the preformed lithium dendrites were not readily expanded by lateral Li deposition, but new dendrites were formed from any defects in the preformed SEI. Such Li deposition should result in the expansion of the Li surface and should accelerate the reaction of the electrolyte and Li metal, lowering the CE, as observed for the Li/Cu and Li/LCO tests. When FEC was added to the control electrolyte at 2 and 10 wt %, the diameters of the lithium dendrites were larger than that of the control (Figure 6b,c). The higher FEC content resulted in thicker lithium dendrites. For the three FEC/DEC electrolytes, thicker lithium dendrites with diameters of around 1 μm were observed (Figure 6d−f). This morphological feature can be understood by considering the LiF and carbonate components in the SEI layers derived from FEC. The Li-ion-conducting LiF components permit Li-ion transport through the SEI layer and the elastic carbonate compound accommodates the resulting volume expansion of Li dendrites. Because the Li-metal surfaces are less expanded and the SEI layers are more stably preserved, electrolytes with relatively high FEC contents can improve the CE and cycling stability.

CONCLUSIONS

High cycling stability of Li/LCO batteries was achieved by tuning FEC-containing electrolytes. Above a certain FEC content, stabilization of Li-metal electrodes was clearly observed. Among the electrolytes investigated, the 1 M LiPF$_6$ 30FEC/70DEC electrolyte showed the highest ionic conductivity and the highest cycling stability for the Li/LCO and Li/Cu cell test. At an FEC content of 50 wt % and above, a considerable reduction of initial discharge capacity was observed because of the formation of a resistive layer on the LCO surface, indicating the existence of an optimum FEC content for the design of LCO-based lithium-metal batteries. The Li/LCO cell with the 30FEC/70DEC electrolyte showed a capacity retention of 97.5% and CE of 99.0% even after 300 cycles, demonstrating the importance of tuning the two interfaces. XPS analysis clearly showed that the FEC-derived SEI layers include LiF and polycarbonates. The diameters of the noodle-like Li deposits observed for the FEC/DEC electrolytes were an order of magnitude larger than those of the EC/DEC electrolyte. The resulting Li deposit for the FEC/DEC electrolyte suggests that the resulting SEI layer is ion-conductive and elastic.

EXPERIMENTAL SECTION

Measurement of Ionic Conductivity of the Electrolyte. Ionic conductivity of the electrolyte was determined from ac impedances of an SUS/PP separator/SUS symmetric cell containing electrolyte. The thickness of the PP separator is 20 μm and the diameter of the SUS disc electrode is 0.8 cm. The excess 200 μL of electrolyte is injected to the 2032 type coin cell.

Electrochemical Measurements. Electrochemical performance measurements were carried out using 2032 coin-type cells. Li-metal batteries were assembled in an argon-filled glovebox consisting of the electrodes, a PP separator (PP2400, Celgard, USA), and an electrolyte (PANAX ETEC Co. Ltd, South Korea), and 100 μL of lithium hexafluorophosphate (LiPF$_6$, 1 M) in ethylene carbonate and diethyl carbonate (EC/DEC, 1:1 by volume) was used as the electrolyte for every electrochemical cell test. The LiCoO$_2$ (LCO) cathode was prepared by casting a slurry consisting of 90 wt % LCO (Umicore Co. Ltd, South Korea), 5 wt % SUPER P carbon black (Timcal, Switzerland), 5 wt % polyvinylidene fluoride (Sigma-Aldrich, USA) binder, and N-methyl-2-pyrrolidone as a solvent onto an Al foil. We used the 450 μm thickness of the lithium metal (Honjo Metal), and the areal capacity of the LCO cathode is 1.5 mA h cm^{-2}. Galvanostatic experiments were performed using a battery cycler (WBCS 3000, WonATech, South Korea), and the cells were placed in an environmental chamber in which the temperature was controlled at 25 °C. To examine the performance of the Li/LCO cell, the assembled cells were operated at 0.15 mA cm^{-2} current density for charge and discharge formation cycle and the cell was cycled at 1.5 mA cm^{-2} current density. The cutoff voltages for charging and discharging were 4.2 and 3.0 V versus Li/Li$^+$, respectively. Electrochemical impedance spectra measurements were performed using a Solartron 1255 (Solartron Analytical, UK) frequency response analyzer and a Solartron 1287 electrochemical workstation in the frequency range of 1 MHz to 0.1 Hz with a perturbation amplitude of 10 mV.

Morphological and Chemical Bonding Characterizations. The morphology of the Li-metal electrodes was examined by field-emission SEM (Sirion, FEI). In a dry glovebox filled with argon, the Li-metal electrodes were carefully separated from the disassembled cells after electrochemical investigations. To remove any residual electrolyte, the obtained electrodes were gently rinsed with 1,2-dimethoxyethane (anhydrous, 99.5%, Sigma-Aldrich, USA) and dried under vacuum overnight. The samples were vacuum-sealed in a PP bottle for safe transfer without contamination and exposed to air only for a few seconds at sample loading. To prevent Li-metal contamination, the bonding characterizations of the electrode surface were carried out via FT-IR (IFS66V/S-HYPERION 300, Bruker Optic) and XPS (Sigma Probe, Thermo VG Scientific) in a vacuum chamber. The FT-IR analysis was carried out in the wave number range of 2000–900 cm^{-1}, and XPS spectra were calibrated against the hydrocarbon peak at a binding energy of 285.0 eV.

ASSOCIATED CONTENT

Ⓢ Supporting Information

The Supporting Information is available free of charge on the ACS Publications website at DOI: 10.1021/acsomega.8b03022.

XPS survey scan and atomic contents percentage of the Li metal and LCO cathode, FT-IR spectra of the cathode surface, the Nyquist plot of impedance of various electrolytes, the contact angle of electrolytes on the PP separator, CE of the Li–Cu cell, and 3-electrode impedance data of Li/LCO (PDF)

AUTHOR INFORMATION

Corresponding Author

*E-mail: heetak.kim@kaist.ac.kr (H.-T.K.). Phone: +82-42-350-3916. Fax: +82-42-350-3910.

ORCID Ⓞ

Hongkyung Lee: 0000-0002-7732-2089
Hee-Tak Kim: 0000-0003-4578-5422

Notes

The authors declare no competing financial interest.

ACKNOWLEDGMENTS

REFERENCES

(1) Xu, W.; Wang, J.; Ding, F.; Chen, X.; Nasybulin, E.; Zhang, Y.; Zhang, J.-G. Lithium metal anodes for rechargeable batteries. *Energy Environ. Sci.* **2014**, 7, 513−537.

(2) Lu, Y.; Tu, Z.; Archer, L. A. Stable lithium electrodeposition in liquid and nanoporous solid electrolytes. *Nat. Mater.* **2014**, 13, 961−969.

(3) Yan, K.; Lu, Z.; Lee, H.-W.; Xiong, F.; Hsu, P.-C.; Li, Y.; Zhao, J.; Chu, S.; Cui, Y. Selective deposition and stable encapsulation of lithium through heterogeneous seeded growth. *Nat. Energy* **2016**, 1, 16010.

(4) Lin, D.; Liu, Y.; Liang, Z.; Lee, H.-W.; Sun, J.; Wang, H.; Yan, K.; Xie, J.; Cui, Y. Layered reduced graphene oxide with nanoscale interlayer gaps as a stable host for lithium metal anodes. *Nat. Nanotechnol.* **2016**, 11, 626−632.

(5) Evers, S.; Nazar, L. F. New Approaches for High Energy Density Lithium-Sulfur Battery Cathodes. *Acc. Chem. Res.* **2012**, 46, 1135−1143.

(6) Ji, X.; Nazar, L. F. Advances in Li-S batteries. *J. Mater. Chem.* **2010**, *20*, 9821−9826.

(7) Bruce, P. G.; Freunberger, S. A.; Hardwick, L. J.; Tarascon, J.-M. Li-O₂ and Li-S batteries with high energy storage. *Nat. Mater.* **2012**, *11*, 19−29.

(8) Hardwick, L. J.; Bruce, P. G. The pursuit of rechargeable non-aqueous lithium-oxygen battery cathodes. *Curr. Opin. Solid State Mater. Sci.* **2012**, *16*, 178−185.

(9) Tarascon, J.-M.; Armand, M. Issues and challenges facing rechargeable lithium batteries. *Nature* **2001**, *414*, 359−367.

(10) Scrosati, B.; Garche, J. Lithium batteries: Status, prospects and future. *J. Power Sources* **2010**, *195*, 2419−2430.

(11) Aurbach, D. Review of selected electrode-solution interactions which determine the performance of Li and Li ion batteries. *J. Power Sources* **2000**, *89*, 206−218.

(12) López, C. M.; Vaughey, J. T.; Dees, D. W. Morphological transitions on lithium metal anodes. *J. Electrochem. Soc.* **2009**, *156*, A726−A729.

(13) Lu, D.; Shao, Y.; Lozano, T.; Bennett, W. D.; Graff, G. L.; Polzin, B.; Zhang, J.; Engelhard, M. H.; Saenz, N. T.; Henderson, W. A.; Bhattacharya, P.; Liu, J.; Xiao, J. Failure Mechanism for Fast-Charged Lithium Metal Batteries with Liquid Electrolytes. *Adv. Energy Mater.* **2014**, *5*, 1400993.

(14) Zhamu, A.; Chen, G.; Liu, C.; Neff, D.; Fang, Q.; Yu, Z.; Xiong, W.; Wang, Y.; Wang, X.; Jang, B. Z. Reviving rechargeable lithium metal batteries: enabling next-generation high-energy and high-power cells. *Energy Environ. Sci.* **2012**, *5*, 5701−5707.

(15) Liu, Y.; Lin, D.; Liang, Z.; Zhao, J.; Yan, K.; Cui, Y. Lithium-coated polymeric matrix as a minimum volume-change and dendrite-free lithium metal anode. *Nat. Commun.* **2016**, *7*, 10992.

(16) Selis, L. A.; Seminario, J. M. Dendrite formation in silicon anodes of lithium-ion batteries. *RSC Adv.* **2018**, *8*, 5255−5267.

(17) Cheng, X.-B.; Zhang, R.; Zhao, C.-Z.; Wei, F.; Zhang, J.-G.; Zhang, Q. A review of solid electrolyte interphases on lithium metal anode. *Adv. Sci.* **2015**, *3*, 1500213.

(18) Lee, J. T.; Nitta, N.; Benson, J.; Magasinski, A.; Fuller, T. F.; Yushin, G. Comparative study of the solid electrolyte interphase on graphite in full Li-ion battery cells using X-ray photoelectron spectroscopy, secondary ion mass spectrometry, and electron microscopy. *Carbon* **2013**, *52*, 388−397.

(19) Lee, H.; Lee, D. J.; Kim, Y.-J.; Park, J.-K.; Kim, H.-T. A simple composite protective layer coating that enhances the cycling stability of lithium metal batteries. *J. Power Sources* **2015**, *284*, 103−108.

(20) Tu, Z.; Kambe, Y.; Lu, Y.; Archer, L. A. Nanoporous Polymer-Ceramic Composite Electrolytes for Lithium Metal Batteries. *Adv. Energy Mater.* **2014**, *4*, 1300654.

(21) Choudhury, S.; Mangal, R.; Agrawal, A.; Archer, L. A. A highly reversible room-temperature lithium metal battery based on cross-linked hairy nanoparticles. *Nat. Commun.* **2015**, *6*, 10101.

(22) Zhou, W.; Wang, S.; Li, Y.; Xin, S.; Manthiram, A.; Goodenough, J. B. Plating a dendrite-free lithium anode with a polymer/ceramic/polymer sandwich electrolyte. *J. Am. Chem. Soc.* **2016**, *138*, 9385−9388.

(23) Yan, K.; Lee, H.-W.; Gao, T.; Zheng, G.; Yao, H.; Wang, H.; Lu, Z.; Zhou, Y.; Liang, Z.; Liu, Z.; Chu, S.; Cui, Y. Ultrathin two-dimensional atomic crystals as stable interfacial layer for improvement of lithium metal anode. *Nano Lett.* **2014**, *14*, 6016−6022.

(24) Choi, N.-S.; Yew, K. H.; Lee, K. Y.; Sung, M.; Kim, H.; Kim, S.-S. Effect of fluoroethylene carbonate additive on interfacial properties of silicon thin-film electrode. *J. Power Sources* **2006**, *161*, 1254−1259.

(25) Chen, L.; Wang, K.; Xie, X.; Xie, J. Enhancing electrochemical performance of silicon film anode by vinylene carbonate electrolyte additive. *Electrochem. Solid-State Lett.* **2006**, *9*, A512−A515.

(26) Xiong, S.; Xie, K.; Diao, Y.; Hong, X. Properties of surface film on lithium anode with LiNO₃ as lithium salt in electrolyte solution for lithium−sulfur batteries. *Electrochim. Acta* **2012**, *83*, 78−86.

(27) Li, W.; Yao, H.; Yan, K.; Zheng, G.; Liang, Z.; Chiang, Y.-M.; Cui, Y. The synergetic effect of lithium polysulfide and lithium nitrate to prevent lithium dendrite growth. *Nat. Commun.* **2015**, *6*, 7436.

(28) Lin, Y.-M.; Klavetter, K. C.; Abel, P. R.; Davy, N. C.; Snider, J. L.; Heller, A.; Mullins, C. B. High performance silicon nanoparticle anode in fluoroethylene carbonate-based electrolyte for Li-ion batteries. *Chem. Commun.* **2012**, *48*, 7268−7270.

(29) Shin, H.; Park, J.; Sastry, A. M.; Lu, W. Effects of fluoroethylene carbonate (FEC) on anode and cathode interfaces at elevated temperatures. *J. Electrochem. Soc.* **2015**, *162*, A1683−A1692.

(30) Zhang, X.-Q.; Cheng, X.-B.; Chen, X.; Yan, C.; Zhang, Q. Fluoroethylene carbonate additives to render uniform Li deposits in lithium metal batteries. *Adv. Funct. Mater.* **2017**, *27*, 1605989.

(31) Zhang, X.-Q.; Chen, X.; Cheng, X.-B.; Li, B.-Q.; Shen, X.; Yan, C.; Huang, J.-Q.; Zhang, Q. Highly stable lithium metal batteries enabled by regulating the solvation of lithium ions in nonaqueous electrolytes. *Angew. Chem., Int. Ed.* **2018**, *57*, 5301−5305.

(32) Etacheri, V.; Haik, O.; Goffer, Y.; Roberts, G. A.; Stefan, I. C.; Fasching, R.; Aurbach, D. Effect of fluoroethylene carbonate (FEC) on the performance and surface chemistry of Si-nanowire Li-ion battery anodes. *Langmuir* **2011**, *28*, 965−976.

(33) Markevich, E.; Salitra, G.; Chesneau, F.; Schmidt, M.; Aurbach, D. Very Stable Lithium Metal Stripping-Plating at a High Rate and High Areal Capacity in Fluoroethylene Carbonate-Based Organic Electrolyte Solution. *ACS Energy Lett.* **2017**, *2*, 1321−1326.

(34) Salitra, G.; Markevich, E.; Afri, M.; Talyosef, Y.; Hartmann, P.; Kulisch, J.; Sun, Y.-K.; Aurbach, D. High-Performance Cells Containing Lithium Metal Anodes, LiNi0.6Co0.2Mn0.2O2 (NCM 622) Cathodes, and Fluoroethylene Carbonate-Based Electrolyte Solution with Practical Loading. *ACS Appl. Mater. Interfaces* **2018**, *10*, 19773−19782.

(35) Okuno, Y.; Ushirogata, K.; Sodeyama, K.; Tateyama, Y. Decomposition of the fluoroethylene carbonate additive and the glue effect of lithium fluoride products for the solid electrolyte interphase: an ab initio study. *Phys. Chem. Chem. Phys.* **2016**, *18*, 8643−8653.

(36) Borodin, O.; Olguin, M.; Spear, C. E.; Leiter, K. W.; Knap, J. Towards high throughput screening of electrochemical stability of battery electrolytes. *Nanotechnology* **2015**, *26*, 354003.

(37) Li, Y.; Lian, F.; Ma, L.; Liu, C.; Yang, L.; Sun, X.; Chou, K. Fluoroethylene Carbonate as Electrolyte Additive for Improving the electrochemical performances of High-Capacity Li1.16-[Mn0.75Ni0.25]0.84O2 Material. *Electrochim. Acta* **2015**, *168*, 261−270.

(38) Liu, H.; Hou, P.; Zhang, W.; Kim, Y. K.; Wu, J. The synthesis and characterization of polymer-coated FeAu multifunctional nano-particles. *Nanotechnology* **2010**, *21*, 335602.

(39) Xu, K. Nonaqueous liquid electrolytes for lithium-based rechargeable batteries. *Chem. Rev.* **2004**, *104*, 4303−4418.

(40) Kim, Y.-J.; Lee, H.; Noh, H.; Lee, J.; Kim, S.; Ryou, M.-H.; Lee, Y. M.; Kim, H.-T. Enhancing the Cycling Stability of Sodium Metal Electrodes by Building an Inorganic-Organic Composite Protective Layer. *ACS Appl. Mater. Interfaces* **2017**, *9*, 6000−6006.

(41) Aktekin, B.; Younesi, R.; Zipprich, W.; Tengstedt, C.; Brandell, D.; Edström, K. The Effect of the Fluoroethylene Carbonate Additive in LiNi0.5Mn1.5O4- Li4Ti5O12Lithium-Ion Cells. *J. Electrochem. Soc.* **2017**, *164*, A942−A948.

(42) Song, J.; Lee, H.; Wang, Y.; Wan, C. Two- and three-electrode impedance spectroscopy of lithium-ion batteries. *J. Power Sources* **2002**, *111*, 255−267.

(43) Cho, H.-M.; Park, Y. J.; Yeon, J.-W.; Shin, H.-C. In-Depth Investigation on Two- and Three-Electrode Impedance Measurements in Terms of the Effect of the Counter Electrode. *Electron. Mater. Lett.* **2009**, *5*, 169−178.